HA14-1, but not the BH3 mimetic ABT-737, causes Ca^{2+} dysregulation in platelets and human cell lines

Many Bcl-2-dependent cancer cells are primed to death due to their upregulation of BH3-only proteins in response to ongoing oncogenic stress. BH3-mimetic drugs like ABT-737 compete with Bim for binding to Bcl-2, releasing Bim and triggering Bax/Bak-mediated apoptosis.[1] While ABT-737 causes regression of established tumors,[2] it also limits platelet survival.[3] The mechanisms underlying the observed thrombocytopenia have been the subject of debate. Since Bcl-Xl is essential for platelet life span,[4] it was proposed that ABT-737, which does not discriminate between Bcl-2 and Bcl-Xl,[5] kills platelets by antagonizing Bcl-Xl.[3] However, these devastating effects of ABT-737 on platelet function were also associated with disturbed intracellular Ca^{2+} homeostasis and dynamics,[3] but this remains poorly understood and controversial.[6,7]

We, therefore, explored the effect of ABT-737 on apoptosis in platelets and on intracellular Ca^{2+} signaling in platelets and human cell lines. We compared its effects on Ca^{2+} homeostasis with another Bcl-2 antagonist, the HA14-1 compound, which was reported to exert inhibitory properties on sarco/endoplasmic reticulum Ca^{2+}-ATPases (SERCA).[8] Washed platelets were prepared as described.[9] For this, venous blood was collected from healthy donors. Permission was given by the Ethical Committee of the Leuven University Hospital to use blood from healthy individuals for further analysis. For apoptosis measurements, platelets were incubated with Annexin-V-FITC and analyzed with an Attune® Acoustic Focusing Flow Cytometer (Applied Biosystems). For the Ca^{2+} measurements in intact cells, platelets were seeded the day of

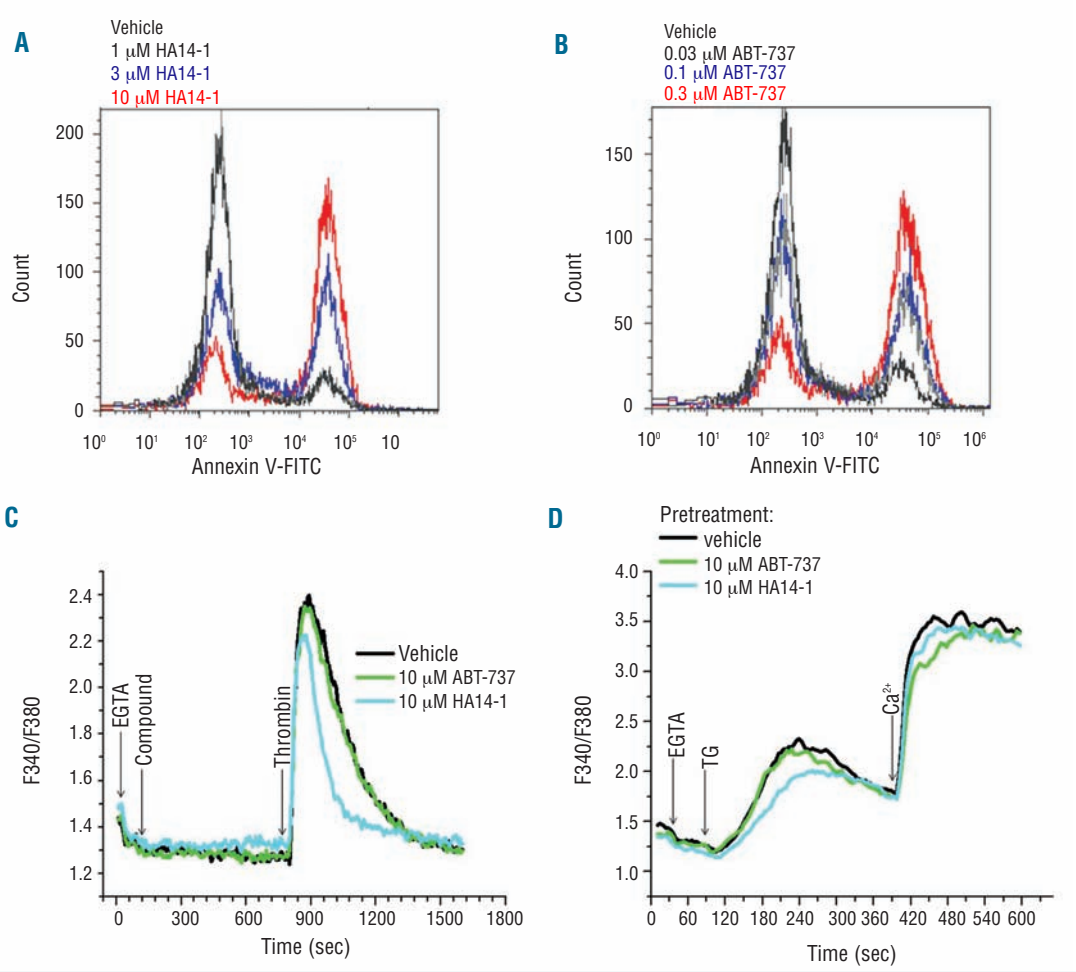

Figure 1. The effect of HA14-1 and ABT-737 on apoptosis and intracellular Ca^{2+} signaling in platelets. (A-B) Flow-cytometry analysis of HA14-1 and ABT-737-induced apoptosis in platelets. (A) Histogram overlay representation of Annexin V-FITC staining of platelets treated for 2 h without (black) or with 1 μM (gray), 3 μM (blue) and 10 μM HA14-1 (red). (B) Histogram overlay representation of Annexin V-FITC staining of platelets treated for 3 h without (black) or with 0.03 μM (gray), 0.1 μM (blue) and 0.3 μM ABT-737 (red). (C-D) Fluorimetric analysis of the ABT-737- and HA14-1-induced Ca^{2+} responses in Fura2-loaded platelets. (C) The ratio of emitted fluorescence of Fura2 (excitation wavelength 340 nm/ 380 nm) was monitored and the different treatments were applied 60 s after the addition of EGTA (3 mM) which prohibits Ca^{2+} entry. The black, green and cyan lines represent Ca^{2+} signals obtained for platelets treated with vehicle, 10 μM ABT-737 or 10 μM HA14-1, respectively. 0.5 U/mL thrombin was added after 760 s as positive control. (D) Analysis of the thapsigargin (TG)-induced Ca^{2+} responses in untreated platelets (black) or following 30 min of pre-treatment without or with 10 μM HA14-1 (cyan) or ABT-737 (green). 10 μM thapsigargin was added 60 s after EGTA (3 mM) addition. Ca^{2+} (3 mM) was added at 400 s in order to show that the Ca^{2+}-influx capacity of the platelets is not affected by any of the different conditions.

measurement in poly-L-lysine-coated 96-well plates (Greiner) at a density of approximately 3 x 10^8 platelets/mL. Ca^{2+} measurements in intact Hela cells and unidirectional $^{45}Ca^{2+}$-flux experiments in permeabilized cells were basically performed as previously described.[10] SERCA2b ATPase activity was determined by colorimetric monitoring[11] in a Ca^{2+}-buffered solution containing microsomes (10 μg of protein) from HEK-293T cells ectopically expressing SERCA2b. Results are expressed as average ± standard deviation (SD). Significance was determined using two-tailed paired Student's t-test. $P<0.05$ was considered significant.

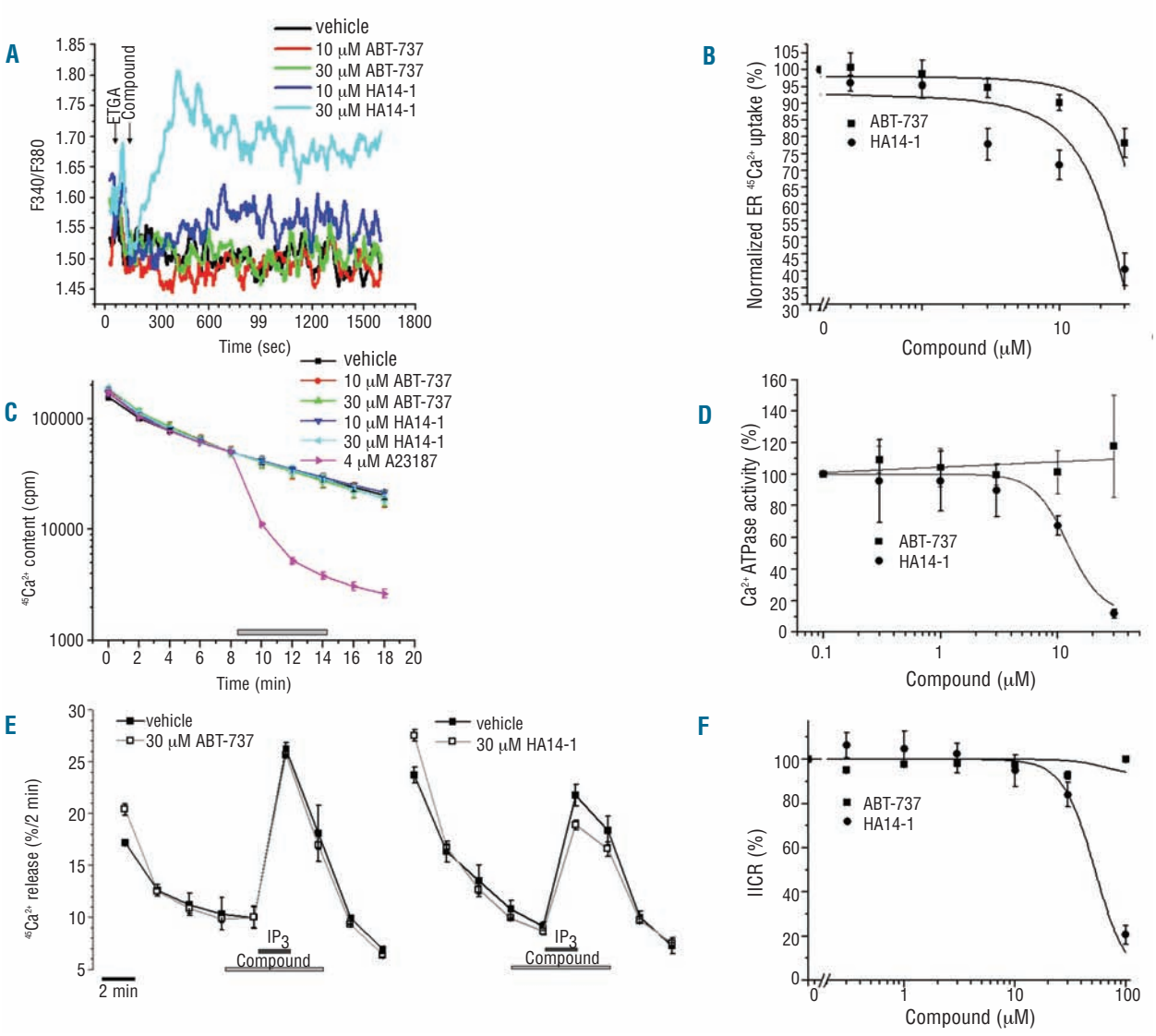

Figure 2. The effect of HA14-1 and ABT-737 on ER Ca^{2+}-uptake and –release mechanisms. (A) Fluorimetric analysis of the HA14-1 and ABT-737-induced Ca^{2+} responses in HeLa cells. The ratio of emitted fluorescence of Fura2 (excitation wavelength 340 nm/380 nm) was monitored and the five different treatments, vehicle, 10 and 30 μM ABT-737, and 10 and 30 μM HA14-1, were added 60 s after the addition of 3 mM EGTA. All curves are representative for 3 independent experiments. (B) Normalized ER $^{45}Ca^{2+}$ uptake values (in %) obtained from permeabilized cells in which steady state ER $^{45}Ca^{2+}$ loading was performed in the presence of different ABT-737 and HA14-1 concentrations. Values for vehicle-treated cells were taken as 100%. Data represent mean ± SEM of 3-5 independent experiments. (C) Effect of vehicle, ABT-737, HA14-1 and A23187 on the unidirectional $^{45}Ca^{2+}$ efflux in the absence of SERCA Ca^{2+}-uptake activity. Data represent the ER Ca^{2+} content (in cpm) as a function of time (in min) and are plotted as mean ± SD. A typical experiment out of 3 independent experiments is shown. (D) Dose response curve of ABT-737 and HA14-1 on normalized SERCA2b activity. SERCA2b ATPase activity was measured at 1 μM Ca^{2+}. ABT-737 does not have any significant effect on the ATPase activity whereas HA14-1 effectively inhibited SERCA2b activity (IC_{50} ~14 μM). (E) Unidirectional $^{45}Ca^{2+}$-flux experiments in HeLa cells demonstrating IP_3-induced Ca^{2+} release in cells exposed to vehicle (closed symbols), 30 μM ABT-737 (open symbols, left panel) and 30 μM HA14-1 (open symbols, right panel), from 2 min before till 2 min after the addition of IP_3, as indicated by the light gray bar. The addition of IP_3 is indicated by the shorter dark gray bar. Representative traces are shown as fractional $^{45}Ca^{2+}$ release (%/2 min) as a function of time (in min). Data represent mean ± SD of duplicate samples. A typical result out of 4 independent experiments is shown. (F) Normalized IP_3-induced $^{45}Ca^{2+}$ release (IICR) from permeabilized cells exposed to 0.3, 1, 3, 10, 30 and 100 μM ABT-737 or HA14-1. Values for vehicle-treated cells were taken as 100%. Data represent mean ± SEM. of 4 independent experiments from 2 to 4 replicates per experiment. HA14-1 but not ABT-737 inhibited IP_3R-mediated Ca^{2+} release (IC_{50} ~50 μM).

We confirmed that both HA14-1 (3 and 10 μM; 2 h) and ABT-737 (0.03, 0.1 and 0.3 μM; 2 h) provoked apoptosis in blood platelets (Figure 1A and B). However, only HA14-1, but not ABT-737, triggered a slow and steady increase in the cytosolic [Ca^{2+}] originating from the intracellular Ca^{2+} stores in Fura2-loaded platelets exposed to extracellular EGTA (Figure 1C). Moreover, pre-treatment (10 μM; 30 min) of HA14-1, but not of ABT-737, reduced the total Ca^{2+} released from the ER in response to thapsigargin, an irreversible SERCA inhibitor, while not affecting store-operated Ca^{2+} influx (Figure 1D). To confirm our result in another cell model, we used the human cell line HeLa. Again, HA14-1, but not ABT-737, affected intracellular Ca^{2+} homeostasis in these cells in a concentration-dependent manner (Figure 2A). To investigate the underlying mechanism, we applied a highly quantitative $^{45}Ca^{2+}$-flux assay[10] in permeabilized HeLa cells to specifically assess ER 45Ca^{2+}-uptake activity in the absence of plasmalemmal and mitochondrial Ca^{2+} fluxes and of IP_3R-mediated Ca^{2+}-release. Application of HA14-1 during the ER $^{45}Ca^{2+}$-loading phase caused a strong decrease in the steady-state 45Ca^{2+} loading levels, while ABT-737 was much less effective (Figure 2B). The steady-state ER Ca^{2+} levels are determined by the balance between the ER Ca^{2+}-uptake and ER Ca^{2+}-leak activities. Importantly, application of either ABT-737 or HA14-1 (up to 30 μM) during the efflux phase did not affect the ER Ca^{2+}-leak rate (Figure 2C), suggesting an inhibition of the ER Ca^{2+}-uptake activity. Next, we directly assessed the effect of ABT-737 and HA14-1 on SERCA2b activity, the housekeeping isoform in human platelets,[12] which was ectopically expressed in HEK-293T cells (Figure 2D). HA14-1 effectively inhibited SERCA2b Ca^{2+} ATPase activity (IC_{50} = 14 μM) while ABT-737 (up to 30 μM) had no effect. Finally, we assessed whether ABT-737 or HA14-1 directly affected IP_3R-mediated Ca^{2+} release (e.g. which occurs in response to thrombin exposure of platelets). We used the $^{45}Ca^{2+}$-flux assay to accurately measure IP_3-induced Ca^{2+} release in permeabilized HeLa cells. We found that 30 μM HA14-1, but not ABT-737, inhibited the IP_3R (Figure 2E). Performing a dose-response curve, we found that ABT-737 up to 100 μM did not inhibit IP_3Rs. In contrast, HA14-1 potently inhibited IP_3Rs at concentrations higher than 10 μM with an IC_{50} of approximately 50 μM and with an IP_3R inhibition of approximately 80% at 100 μM (Figure 2F).

Our experiments clearly indicate that disrupted intracellular Ca^{2+} homeostasis is not a proximal event in ABT-737-induced thrombocytopenia. Thus, earlier studies indicating depleted intracellular Ca^{2+} homeostasis in platelets exposed for 10 μM ABT-737 for prolonged periods (e.g. 2 h) may reflect a late event that is the consequence of Bcl-Xl inhibition and ongoing cell death in platelets.[6]

We conclude that the dysregulation of intracellular Ca^{2+} signaling in platelets and human cell lines by HA14-1 is an off-target effect on SERCA2b and on IP_3Rs, since on-target inhibition of Bcl-2/Bcl-Xl by ABT-737 does not disrupt intracellular Ca^{2+} signaling. Thus, ABT-737 has a safe Ca^{2+}-signaling profile, since ABT-737, at therapeutically relevant concentrations (i.e. below 1 μM), does not affect intracellular Ca^{2+}-transport mechanisms essential for cellular homeostasis.

Haidar Akl,[1] Ilse Vandecaetsbeek,[2] Giovanni Monaco,[1] Alexandre Kauskot,[3] Tomas Luyten,[1] Kirsten Welkenhuyzen,[1] Marc Hoylaerts,[1] Humbert De Smedt,[1] Jan B. Parys,[1] and Geert Bultynck[1]

[1]Laboratory of Molecular and Cellular Signaling and [2]Laboratory of Cellular Transport Systems, Department Cellular and Molecular Medicine, KU Leuven, Leuven; and [3]Center for Molecular and Vascular Biology, KU Leuven, Leuven, Belgium

Correspondence: geert.bultynck@med.kuleuven.be

doi:10.3324/haematol.2012.080598

Key-words: platelets, molecular pharmacology, BH3 mimetic, calcium.

Acknowledgments: we would like to acknowledge Abbott Laboratories who supplied us with ABT-737. We thank Marina Crabbé and Anja Florizoone for excellent technical help and Ludwig Missiaen for helpful discussions.

Funding: this work was supported by the Research Foundation-Flanders (FWO) (grants G.0604.07N to HDS, G.0788.11N to GB and G.0819.13N to GB and HDS), by the Research Council of the KU Leuven via the Concerted Actions program (GOA/09/012) and via an OT-START (STRT1/10/044), by the Interuniversity Attraction Poles Program (Belgian Science Policy; P6/28 to HDS, JBP, LM and GB and P7/13 to JBP, LM and GB), by the Royal Flemish Academy of Belgium for Science and the Arts (Research Award from the Octaaf Dupont Foundation 2010 to GB). HA and GM were supported by the Research Foundation-Flanders (FWO) via a post-doctoral and predoctoral fellowship, respectively.

Information on authorship, contributions, and financial & other disclosures was provided by the authors and is available with the online version of this article at www.haematologica.org.

References

1. Del Gaizo Moore V, Brown JR, Certo M, Love TM, Novina CD, Letai A. Chronic lymphocytic leukemia requires BCL2 to sequester prodeath BIM, explaining sensitivity to BCL2 antagonist ABT-737. J Clin Invest. 2007;117(1):112-21.
2. Oltersdorf T, Elmore SW, Shoemaker AR, Armstrong RC, Augeri DJ, Belli BA, et al. An inhibitor of Bcl-2 family proteins induces regression of solid tumours. Nature. 2005;435(7042):677-81.
3. Vogler M, Hamali HA, Sun XM, Bampton ET, Dinsdale D, Snowden RT, et al. BCL2/BCL-X(L) inhibition induces apoptosis, disrupts cellular calcium homeostasis, and prevents platelet activation. Blood. 2011;117(26):7145-54.
4. Mason KD, Carpinelli MR, Fletcher JI, Collinge JE, Hilton AA, Ellis S, et al. Programmed anuclear cell death delimits platelet life span. Cell. 2007;128(6):1173-86.
5. Chonghaile TN, Letai A. Mimicking the BH3 domain to kill cancer cells. Oncogene. 2008;(27 Suppl 1):S149-57.
6. Harper MT, Poole AW. Bcl-xL-inhibitory BH3 mimetic ABT-737 depletes platelet calcium stores. Blood. 2012;119(18):4337-8.
7. Schoenwaelder SM, Jackson SP. Bcl-xL-inhibitory BH3 mimetics (ABT-737 or ABT-263) and the modulation of cytosolic calcium flux and platelet function. Blood. 2012;119(5):1320-1; author reply 1-2.
8. Hermanson D, Addo SN, Bajer AA, Marchant JS, Das SG, Srinivasan B, et al. Dual mechanisms of sHA 14-1 in inducing cell death through endoplasmic reticulum and mitochondria. Mol Pharmacol. 2009;76(3):667-78.
9. Kauskot A, Di Michele M, Loyen S, Freson K, Verhamme P, Hoylaerts MF. A novel mechanism of sustained platelet αIIbβ3 activation via PEAR1. Blood. 2012;119(17):4056-65.
10. Decuypere JP, Welkenhuyzen K, Luyten T, Ponsaerts R, Dewaele M, Molgo J, et al. Ins(1,4,5)P_3 receptor-mediated Ca^{2+} signaling and autophagy induction are interrelated. Autophagy. 2011;7(12):1472-89.
11. Dode L, Andersen JP, Leslie N, Dhitavat J, Vilsen B, Hovnanian A. Dissection of the functional differences between sarco(endo)plasmic reticulum Ca^{2+}-ATPase (SERCA) 1 and 2 isoforms and characterization of Darier disease (SERCA2) mutants by steady-state and transient kinetic analyses. J Biol Chem. 2003;278(48):47877-89.
12. Juska A, Jardin I, Rosado JA. Physical properties of two types of calcium stores and SERCAs in human platelets. Mol Cell Biochem. 2008;311(1-2):9-18.